Colour Dipole Cascades

Gösta Gustafson[1]

[1]Dept. of Astronomy and Theoretical Physics, Lund University, Lund Sweden

1 The role of pertubation theory and unitarity constraints

HERA has shown that the parton density at small x grows rapidly $\sim 1/x^{1.3}$, as predicted by the perturbative BFKL pomeron. For pp collisions this implies a very large probability for gluon-gluon subcollisions, which implies that unitarity constraints are very important. These constraints lead to saturation of the gluon density, and suppression of partons with $k_\perp < Q_s^2$, which may explain why models based on multiple perturbative partonic subcollisions (like PYTHIA [1, 2]) are very successful at high energies. One can then ask: if perturbative physics dominates, is it then possible to calculate the result from basic principles, without input pdf's?

Unitarity constraints and saturation is most easily described in impact parameter space. Rescattering is represented by a convolution in $\mathbf{k}_\perp$-space, which simplifies to a product in $\mathbf{b}$-space. The small size of $\mathrm{Re}\, A_{el}^{pp}$ indicates that pp interaction is driven by absorption. If the absorption probability in Born approx. equals $2F(b)$, the optical theorem and the eikonal approximation gives the result: $d\sigma_{el}/d^2b = T^2 = (1-e^{-F})^2$, $d\sigma_{tot}/d^2b = 2T = 2(1-e^{-F})$.

2 Dipole cascade evolution

Mueller's dipole cascade model [3, 4] is a formulation of LL BFKL evolution in impact parameter space. A colour charge is always screened by an accompanying anticharge, forming a dipole. The dipole emits bremsstrahlung gluons coherently, which splits the dipole in two dipoles. The new dipoles splits repeatedly, developing into a cascade. When two cascades collide, s-channel unitarity is restored in the eikonal approximation.

The *Lund cascade model, DIPSY* [5–7], is a generalization of Mueller's model. Thus it is based on BFKL evolution, but includes a set of important corrections:

1) Important non-leading effects in BFKL evolution. (The most essential are related to energy conservation and running α_s.)

2) Saturation from pomeron loops in the evolution. (This is not included by Mueller or in the BK equation.)

3) Confinement, which also implies t-channel unitarity.

4) The DIPSY MC gives also fluctuations and correlations.

5) It can be applied to collisions between electrons, protons, and nuclei.

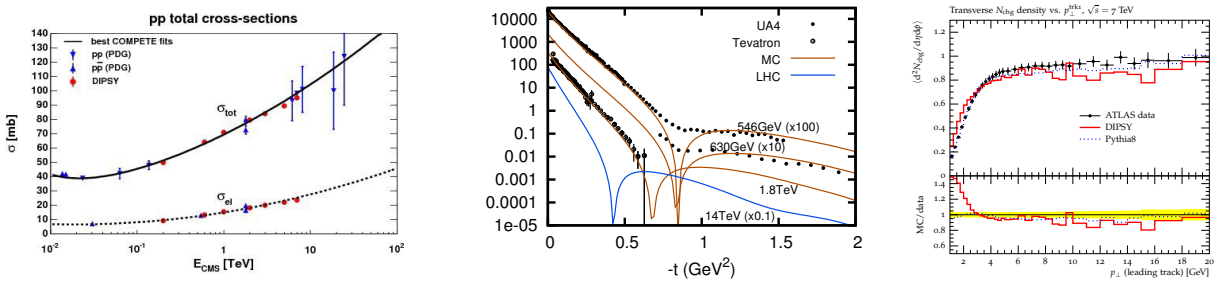

Figure 1: Left: σ_{tot} and σ_{el} vs $\sqrt{s}$. Middle: $d\sigma_{el}/dt$. Right: N_{ch} vs $p_\perp^{lead}$ at 7 TeV. Data from ATLAS.

Some DIPSY results

Cross sections: As examples fig. 1 shows results from DIPSY for the total and elastic pp cross sections. *Note that these results are obtained without input pdf's tuned to experimental data.* The increased cross sections and shrinking forward peak follow directly from the perturbative evolution. As an example for final state properties, N_{ch} vs $p_\perp^{lead}$ is also shown in fig. 1.

Correlations: The BFKL evolution is a stochastic process, and the DIPSY MC can also describe correlations and fluctuations. Results for two-parton correlations are given in ref. [8]. The result depends on both x and Q^2, and a spike (or a hotspot) is developed at larger Q^2 for small transverse separations, corresponding to large momentum imbalance Δ.

Fluctuations and Diffractive excitation

A projectile with a substructure may be diffractively excited to a different mass eigenstate. This can be described in the Good–Walker formalism as the result of fluctuations. Assume that the projectile and the target are linear combinations of diffractive eigenstates, Φ_n, with definite eigenvalues T_n. The elastic amplitude is then given by $\langle\Psi_{in}|T|\Psi_{in}\rangle$, where the average is taken over both projectile and target states. The differential total and elastic cross sections are then given by

$$d\sigma_{tot}/d^2b = 2\langle T\rangle, \quad d\sigma_{el}/d^2b = \langle T\rangle^2.$$

The total diffractive cross section, including elastic scattering, is given by $\langle\, T^2\,\rangle$. Diffractive excitation is obtained subtracting the elastic, and thus given by the fluctuations $\langle\, T^2\,\rangle - \langle T\rangle^2$. For the single and double excitations it is necessary to separate the averages over projectile and target states, below denoted by subscripts p and t respectively. Thus single excitation of the projectile and of the target is given by:

$$d\sigma_{SD,p}/d^2b = \langle\, \langle T\rangle_t^2\,\rangle_p - \langle T\rangle_{p,t}^2, \quad d\sigma_{SD,t}/d^2b = \langle\, \langle T\rangle_p^2\,\rangle_t - \langle T\rangle_{p,t}^2.$$

It is also shown in ref. [9] that the stochastic nature of the BFKL evolution implies that this Good–Walker formalism actually agrees with the more commonly used triple-pomeron analysis.

Fig. 2 shows a comparison between DIPSY and CDF results for single diffraction vs max M_X^2 [10]. It is also possible to calculate diffractive final states. Some results are here also shown in fig. 2 [11]. Note in particular that the MC is here only tuned to $\sigma_{\rm tot}$ and $\sigma_{\rm el}$, with no new parameter.

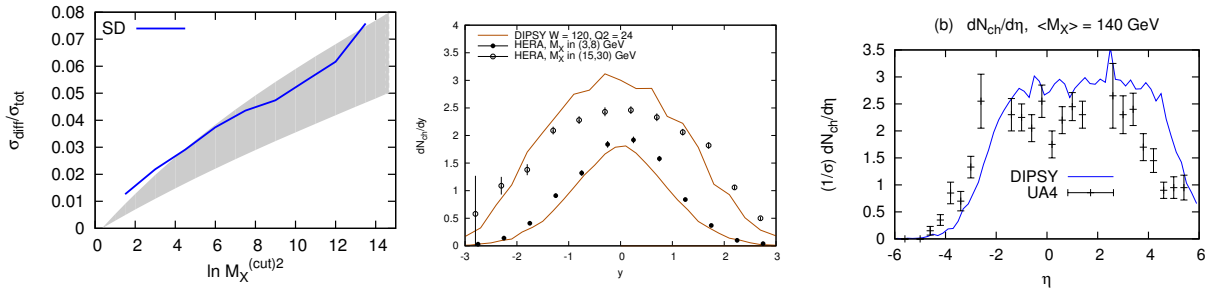

Figure 2: Left: $\int dM_X^2\, d\sigma_{SD}/dM_X^2$ for $M_X < M_X^{(cut)}$. The shaded area is an estimate of CDF results. Middle: $dn_{ch}/d\eta$ in 2 M_X-bins for DIS at $W = 120$ GeV, $Q^2 = 24$ GeV^2. Data from H1. Right: $dn_{ch}/d\eta$ in $p\bar{p}$ collisions at 546 GeV and $\langle M_X \rangle$= 140 GeV. Data from UA4.

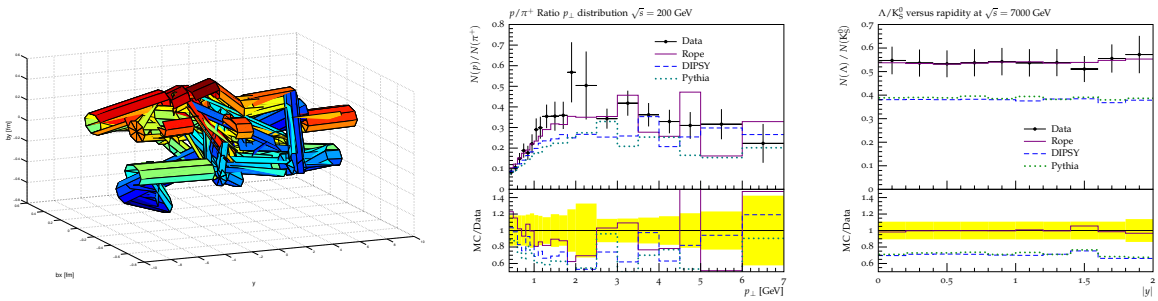

Figure 3: Left: Overlapping strings in $(\mathbf{r}_\perp, y)$-space in pp at 7 TeV. For clarity the radius in the figure is set to 0.1 fm. Middle: p/π ratio at 200 GeV. Right: Λ/K ratio at 7 TeV. Data from STAR and CMS.

3 Final state saturation, Ropes

It has been an old problem that the s/u ratio is higher in pp than in e^+e^- collisions. Also at LHC one observes higher fractions of strange particles and baryons. It was early proposed by Biro, Nielsen, and Knoll [12] that many strings close in transverse space may form "ropes". These authors studied collisions with nuclei, but at high energies there will be many overlapping strings also in pp collisions. This is illustrated in fig. 3, which shows the extension of strings in $(\mathbf{r}_\perp, y)$-space in a pp event at 7 TeV. The string diameter is expected to be of the order of 1 fm, but for a more clear picture, the string radius in fig. 3 is set to 0.1 fm. This shows that there is a very high degree of overlap between the strings.

If overlapping strings interact coherently as a rope, the colour charge at the end of such a rope is obtained from a random walk in colour space. Lattice calculations show that the tension in the rope is then given by the second Casimir operator. In ref. [13] we assume that the rope breaks

by repeated production of $q\bar{q}$ pairs. This implies that the "effective string tension" is determined by the *difference* in rope tension before and after the pair production. The result is a reduction in the number of produced quarks, and a higher rate of strange particles and baryons. Fig. 3 shows some results for p/π and Λ/K ratios.

4 Collisions with nuclei

The DIPSY model is directly generalizable to collisions with nuclei. It here gives a full partonic picture, a dense gluon soup. The model accounts for saturation in the cascades, correlations and fluctuations in the partonic states, and finite size effects. Understanding the initial states is essential for the interpretation of collective final state effects, and models for initial states in AA collisions can be tested in pA or γ^*A. While the nucleus is rather transparent in γ^*A, it is more absorptive in pA. Thus the pA cross section scales approximately with the interaction area $\propto (A^{1/3}+1)^2$ [14]. It is also seen that the colour interference between different nucleons in the nucleus is a small effect in the almost black pA total cross section, but an order 10% effect in γ^*Au, which is more transparent.

Interpreting results for pA collisions, it is interesting to estimate the number of interacting "wounded" nucleons. Gribov showed early that diffractive excitation of the nucleons is important in such an analysis, and it is important to separate the absorptive, non-diffractive, from the inelastic cross section. Diffractive excitation is here most easily treated in the Good–Walker formalism. In many analyses the problem with diffraction is neglected. To our knowledge, also those who include it take only excitation of the projectile into account. A study of the fluctuations causing the excitations, including also effects of excitation of target nucleons, is in progress.

References

[1] Torbjorn Sjostrand and Maria van Zijl, *Phys. Lett.*, **B188**(1987), 149.

[2] Torbjorn Sjostrand, *et al.*, *Comput. Phys. Commun.*, **191**(2015), 159, 1410.3012.

[3] Alfred H. Mueller, *Nucl. Phys.*, **B415**(1994), 373.

[4] Alfred H. Mueller and Bimal Patel, *Nucl. Phys.*, **B425**(1994), 471, hep-ph/9403256.

[5] Emil Avsar, Gosta Gustafson, and Leif Lonnblad, *JHEP*, **07**(2005), 062, hep-ph/0503181.

[6] Emil Avsar, Gosta Gustafson, and Leif Lonnblad, *JHEP*, **01**(2007), 012, hep-ph/0610157.

[7] Christoffer Flensburg, Gosta Gustafson, and Leif Lonnblad, *JHEP*, **08**(2011), 103, 1103.4321.

[8] Ch. Flensburg, G. Gustafson, L. Lonnblad, and A. Ster, *JHEP*, **06**(2011), 066, 1103.4320.

[9] Gosta Gustafson, *Phys. Lett.*, **B718**(2013), 1054, 1206.1733.

[10] Christoffer Flensburg and Gosta Gustafson, *JHEP*, **10**(2010), 014, 1004.5502.

[11] Christoffer Flensburg, Gosta Gustafson, and Leif Lonnblad, *JHEP*, **12**(2012), 115, 1210.2407.

[12] T. S. Biro, Holger Bech Nielsen, and Joern Knoll, *Nucl. Phys.*, **B245**(1984), 449.

[13] Ch. Bierlich, G. Gustafson, L. Lonnblad, and A. Tarasov, *JHEP*, **03**(2015), 148, 1412.6259.

[14] G. Gustafson, L. Lonnblad, A. Ster, and T. Csorgo, *JHEP*, **10**(2015), 022, 1506.09095.